Thermal fluctuation and $1/f$ noise in oriented and unoriented $Y_1Ba_2Cu_3O_{7-x}$ films

R. D. Black, L. G. Turner, A. Mogro-Campero, and T. C. McGee
General Electric Research and Development Center, Schenectady, New York 12301

A. L. Robinson
Department of Electrical Engineering and Computer Science, University of Michigan, Ann Arbor, Michigan 48109-2122

We report on electrical noise measurements made on YBCO ($Y_1Ba_2Cu_3O_{7-x}$) films on $SrTiO_3$, on bulk silicon with a ZrO_2 buffer layer, and on thin dielectric membranes. We have found that $1/f$ noise predominates in the unoriented films and that thermal fluctuation noise is the chief source of noise in good films on $SrTiO_3$.

There have been many recent papers that discuss the use of high-temperature superconductors (HTSs) as detectors of infrared radiation[1-4] and there is some debate as to when and if a nonequilibrium optical response dominates the equilibrium (bolometric) response.[5] Apart from the discussion of the nature of the photo response is the question of the amount of intrinsic electrical noise that occurs in HTS materials and whether it puts limits on the sensitivity of infrared detectors. We have measured the noise in oriented and unoriented ($Y_1Ba_2Cu_3O_{7-x}$) films as a function of temperature and have focused on the noise in the transition region.

We have seen three types of noise in YBCO films. Johnson or Nyquist noise occurs in any material that has a nonzero temperature and resistance and is well understood in the context of equilibrium thermodynamics.[6,7] Thermal fluctuation noise depends on temperature and heat capacity and may also be derived from equilibrium thermodynamics.[8] $1/f$ noise has different origins in different systems[9] and so is perhaps the worst kind of noise from a technological standpoint. $1/f$ noise is particularly baneful in granular systems and unoriented YBCO is no exception.

All of the films in this study were formed by the coevaporation of Y, BaF_2, and Cu. Depositions were done at the ambient temperature of the substrate holder and samples on $SrTiO_3$ were then annealed at 850 °C for 3.5 h in oxygen and water vapor. Samples on other substrates were annealed at 875 °C for 2 h. During the furnace cooling the samples were held at 550 °C for about 0.5 h. The films on $SrTiO_3$ are about 0.25 μm thick and those on bulk silicon and membranes are about 0.9 μm thick. The films on bulk silicon and dielectric membranes have a 0.5-μm-thick buffer layer of ZrO_2 that was evaporated before the YBCO deposition without breaking vacuum. Thin films of YBCO evaporated onto zirconia buffer layers have been shown to be composed of unaligned grains,[10] whereas our YBCO films evaporated onto $SrTiO_3$ are epitaxial.[11]

The dielectric membranes consist of a trilayer of thermal oxide (0.2 μm), low-pressure chemical vapor deposited (LPCVD) nitride (0.12 μm), and LPCVD oxide (0.6 μm). A high-concentration, diffused layer of boron served as an etch stop for the ethylenediamine-pyrocatechol-water etchant that was used to thin the silicon wafer from the back side.[12] The etching step leaves about 5 μm of silicon that can be subsequently removed by a dry etching procedure. We did not remove the remainder of the silicon in this case, however, and so the resultant membrane has this silicon layer as well as the dielectrics mentioned above.

Standard photolithographic techniques were used to pattern the films and a 0.01 normal solution of nitric acid was used to etch them. The silicon samples were in the shape of a meandering line (~55 μm wide in the case of the bulk silicon substrate and ~35 μm wide in the case of the membrane samples). The films on $SrTiO_3$ were patterned and etched into a cross shape that is useful for measuring the isotropy of local resistance fluctuations (not discussed in this paper) and the smallest constrictions are about 12 μm. The evaporated silver (1 μm thick) contacts were annealed at 550 °C for 0.5 h. The samples were mounted in ceramic packages and an ultrasonic lead bonder was used to connect aluminum wires from the contact pads to the package. These contacts proved to be noiseless in subsequent measurements.

Batteries were used in series with a wire wound resistor to provide a constant current to the samples (the value of the series resistor was at least ten times the sample resistance). The voltage leads of the sample went to a low-frequency matching transformer and the output of that transformer went to a PAR 113 low-noise amplifier. The amplified voltage time series went to an HP 3562A spectrum analyzer, where the power spectral density of the noise was computed. The temperature of the samples was controlled by placing them in a Janis Research 10DT supervaritemp liquid-helium cryostat. The flow rate of the helium gas was kept low and the cryostat was placed on a vibration isolation table to prevent microphonic noise.

Figure 1 shows resistance versus temperature (R vs T) curves for the three types of samples that we studied. The resistor on the bulk silicon substrate was somewhat wider than that on the membrane substrate and so the normal-state resistance is somewhat lower. The longer tail in Fig. 1(b) is due to the use of a higher current density for the measurement and to a general softening of the transition due to patterning (due to the inhomogeneity of the material or the effect of the etchant on the grain boundaries). The resistor on $SrTiO_3$ is clearly much more ideal in terms of its metallic behavior in the normal state and in terms of the width of its transition (even with a current density of about 10^5 A/cm²).

FIG. 3. Normalized power spectral density $[(V^2/Hz)/V_{dc}^2]$ vs frequency for the membrane sample.
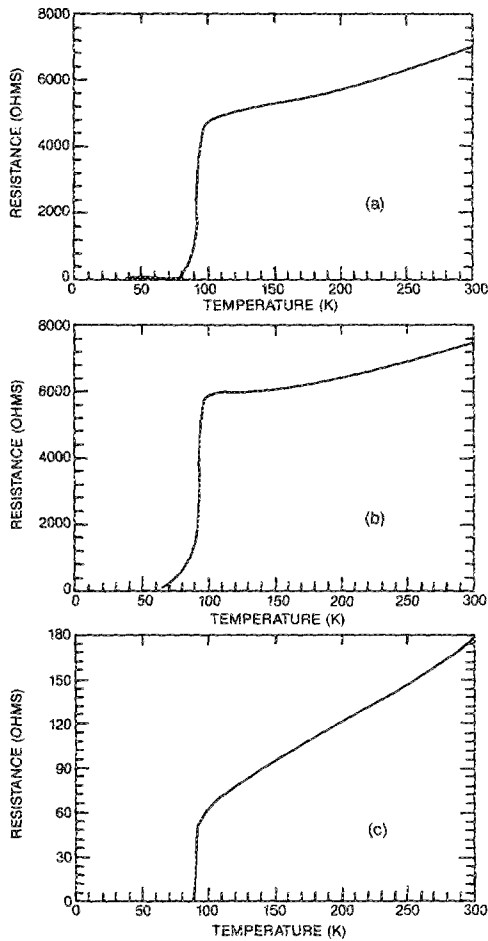
FIG. 1. Resistance vs temperature plots for a YBCO resistor on (a) bulk silicon with a ZrO_2 buffer layer, (b) a dielectric membrane, and (c) bulk $SrTiO_3$ [(100) single crystal].

The R vs T curves were taken with the same current densities as those used for the noise measurements.

Figures 2–4 show normalized noise magnitudes for the three types of samples. The spectra have had a background subtraction (to eliminate amplifier and Johnson noise), were normalized by the square of the dc voltage drop, and were adjusted for the transfer function of the amplifier and matching transformer (the transformer passed frequencies
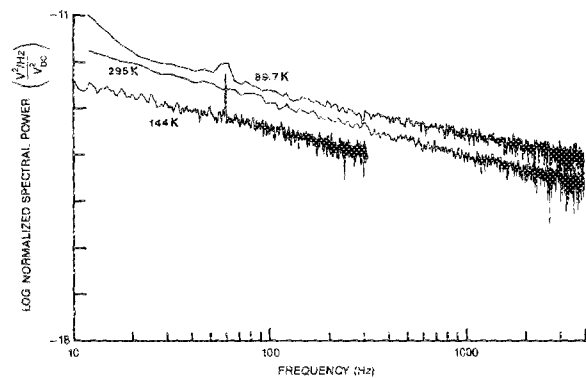
between 3 and 4000 Hz). There was a good deal of low-frequency noise (<20 Hz) that showed up at lower temperatures with and without a dc bias applied to the sample. We suspect that this was due to the modulation of a thermo-electric voltage by vibrations internal to the cryostat. One can also see contamination due to 60 Hz and harmonics of 60 Hz. The noise power scaled as the square of the current.

Figure 2 shows normalized noise spectra for three different temperatures for the bulk silicon substrate sample. The fitted slopes are essentially $1/f$ for each curve. The reduction in noise in going from 295 to 144 K may be due to different stresses in this sample (the other types do not show a noticeable reduction). Note that the noise rises in the transition region (89.7 K) but that it still has a $1/f$ slope.

Figure 3 shows normalized noise spectra for the membrane substrate sample. Again, the noise rises in the transition region but there is no change in slope as compared to the higher temperature measurements. The good match in noise magnitude between this sample and the bulk silicon sample gives us confidence that the flexible membrane did not cause noise-producing cracks in the YBCO film. This is rather remarkable considering the floppiness of the membrane and the tensile stress that it incurred during cooling.

Figure 4 shows normalized noise spectra for the bulk $SrTiO_3$ sample. The great reduction in the magnitude of the $1/f$ noise at temperatures above the transition temperature is clear. Just as in the unoriented film samples the noise magni-

FIG. 2. Normalized power spectral density $[(V^2/Hz)/V_{dc}^2]$ vs frequency for the bulk silicon substrate sample.

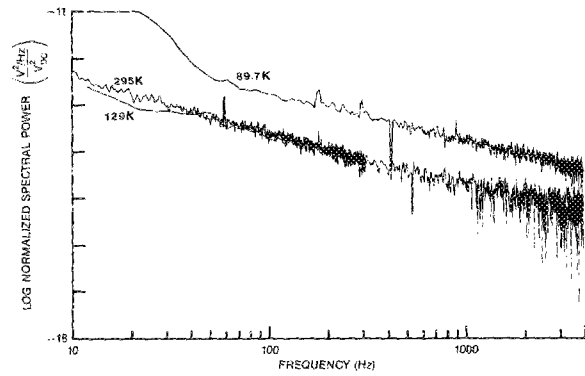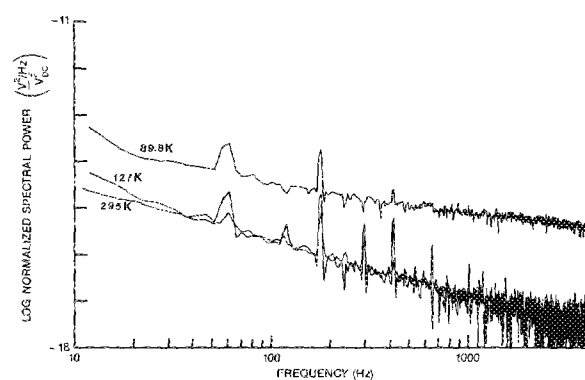FIG. 4. Normalized power spectral density $[(V^2/Hz)/V_{dc}^2]$ vs frequency for the bulk $SrTiO_3$ sample.
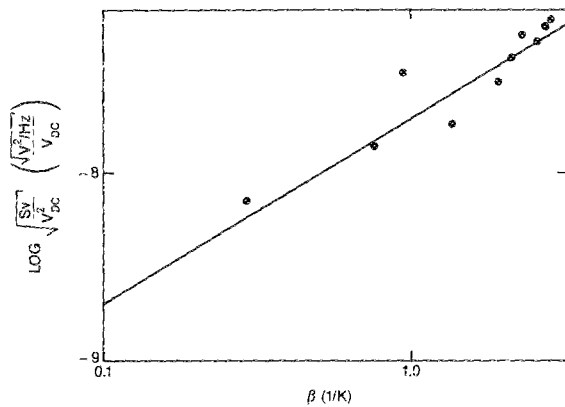
FIG. 5. Square root of normalized power spectral density vs β at 1170 Hz for the bulk SrTiO$_3$ sample. The temperature span is 89.3–90.5 K.

The dominance of thermal fluctuation noise in low-temperature superconducting (LTS) films has been convincingly demonstrated.[14] (That study looked at freely supported films. We are not aware of a study in which epitaxial LTS films have been studied.) The usual Langevin treatment[15] of thermal fluctuation noise predicts a β^2 dependence of the spectral power and predicts certain spectral slopes depending on the geometry of the sample and the bandwidth. In fact, an $f^{-0.5}$ slope is one of the asymptotic limits that comes from this development but a proper treatment of the boundary conditions present in our sample has not yielded a tractable analytic problem. It is not clear what role, if any, flux motion is playing in our result. It is not expected, however, that flux flow noise[16] would have a particular β dependence.

tude rises in the transition region but in this case there is a clear change in the spectral slope. A fit to the slope shows it to go as f^{-a} where $a = 0.53$–0.57. Figure 5 shows the square root of the normalized spectral power versus β ($1/R \times dR/dt$) in the transition region (points taken at 1170 Hz). An identical plot was made using a current density one-half as large as that used for Fig. 5. A numerical fit to these plots shows a linear relationship (that is, spectral power goes as β^2). The results of Figs. 4 and 5 suggest that we are seeing thermal fluctuation noise in the transition region of the SrTiO$_3$ substrate films, unlike the results reported in another recent experiment.[13]

It is clear that unoriented YBCO films are dominated by $1/f$ noise at all temperatures (as long as the resistance is nonzero) and it appears that well oriented films on SrTiO$_3$ exhibit thermal fluctuation noise in the transition region.

$1/f$ noise is very common in granular systems and there is no need to posit unusual mechanisms to explain its presence in unoriented YBCO films. The rise in the normalized magnitude in the transition region seen in Figs. 2 and 3 is due to larger fractional fluctuations in resistance. This is easily explained since the grain boundaries dominate the resistance in the transition region and the resistance fluctuations ($1/f$ noise) are being generated at those boundaries.

[1] P. L. Richards, J. Clarke, R. Leoni, Ph. Lerch, S. Verghese, M. R. Beasley, T. H. Geballe, R. H. Hammond, P. Rosenthal, and S. R. Spielman, Appl. Phys. Lett. 54, 283 (1989).
[2] J. C. Culbertson, U. Strom, S. A. Wolf, P. Skeath, E. J. West, and W. K. Burns, Phys. Rev. B 39, 12359 (1989).
[3] W. S. Brocklesby, D. Monroe, A. F. J. Levi, M. Hong, S. H. Kiou, J. Kwo, C. E. Rice, P. M. Mankiewich, and R. E. Howard, Appl. Phys. Lett. 54, 1175 (1989).
[4] J. Talvacchio, M. G. Forrester, and A. I. Braginski, in Science and Technology of Superconductors, edited by R. McConnell and S. A. Wolf (Plenum, New York, 1989).
[5] E. Zeldov, N. M. Amer, G. Koren, A. Gupta, R. J. Gambino, and M. W. McElfresh, Phys. Rev. Lett. 62, 3093 (1989).
[6] J. B. Johnson, Phys. Rev. 32, 97 (1928).
[7] H. Nyquist, Phys. Rev. 32, 110 (1928).
[8] J. W. Gibbs, Elementary Principles in Statistical Mechanics (Yale University, New Haven, 1902).
[9] M. B. Weissman, Rev. Mod. Phys. 60, 537 (1988).
[10] A. Mogro-Campero, L. G. Turner, E. L. Hall, and M. C. Burrell, Appl. Phys. Lett. 52, 2068 (1988).
[11] A. Mogro-Campero, L. G. Turner, and E. L. Hall, J. Appl. Phys. 65, 4951 (1989).
[12] I. H. Choi and K. D. Wise, Trans. Electron. Devices ED-33, 72 (1986).
[13] P. Rosenthal, R. H. Hammond, M. R. Beasley, R. Leoni, Ph. Lerch, and J. Clarke, IEEE Trans. Magn. MAG-25, 973 (1989).
[14] M. B. Ketchen and J. Clarke, Phys. Rev. B 17, 114 (1978).
[15] R. F. Voss and J. Clarke, Phys. Rev. B 13, 556 (1976).
[16] J. R. Clem, Phys. Rep. 75, 1 (1981).